Polymer Chemistry

PAPER

View Article Online
View Journal | View Issue

Cite this: *Polym. Chem.*, 2018, **9**, 4364

High-performance electrofluorochromic devices based on aromatic polyamides with AIE-active tetraphenylethene and electro-active triphenylamine moieties†

Shun-Wen Cheng,‡[a] Ting Han, ‡[b] Teng-Yung Huang,[a] Ben-Zhong Tang*[b] and Guey-Sheng Liou *[a,c]

Received 1st June 2018,
Accepted 27th July 2018

DOI: 10.1039/c8py00809d

rsc.li/polymers

Novel electrochromic (EC) and aggregation-enhanced emission (AEE)-active triphenylamine (TPA)-based polyamides were prepared with 4-cyanotriphenylamine (**TPA-CN**), 4-methoxytriphenylamine (**TPA-OMe**), cyclohexane (CH) and tetraphenylethene (TPE) moieties *via* condensation polymerization. The emission from the polyamides could be quenched from the neutral to oxidized states effectively due to the structural planarization and optical absorption shift of TPA units during electrochemical switching. With the introduction of *n*-heptyl viologen (HV) into the device system as a counter EC layer for balancing charges, the resulting high-performance electrofluorochromic (EFC) devices based on **TPA-CN-CH** as a photoluminescent (with a fluorescence quantum yield of up to 46% in the film state) and redox-active layer showed a high fluorescence contrast ratio (I_{off}/I_{on}) of 105. The HV-containing **TPA-OMe-TPE**-based EFC device displayed the shortest response time of less than 4.9 s, and excellent improvement in reducing the switching recovery time and lowering the oxidation potential could also be achieved. Thus, judiciously designed multi-functional polymers with both redox- and AEE-active features are a crucial and feasible approach for preparing highly efficient EFC devices.

Introduction

Luminescent materials with efficient solid-state luminescence have attracted a great deal of attention due to their rapid development and great potential for applications in fluorescent biosensors, bioimaging, organic light emitting diodes (OLEDs) and other optoelectronic devices. However, the spontaneous aggregation process of conventional luminogens often suffers from the aggregation-caused quenching (ACQ) effect, which limits their further practical applications. Aggregation-induced emission (AIE) or aggregation-enhanced emission (AEE) is a totally different luminescence phenomenon from ACQ.[1,2] Luminescent materials with AIE/AEE characteristics show a much stronger light emission upon aggregation. Therefore, they can be used as efficient solid-state light emitters in various applications.[3,4] Photoluminescence (PL) is an attractive property for electroactive materials. Another interesting behaviour for electroactive materials is that they can produce different optical absorption bands during electrochemical redox reactions with color changes between the transparent neutral state and the colored switching state. Such coloration was first termed electrochromism by Platt in 1961.[5] Afterwards, a large amount of electrochromic (EC) materials for fabricating EC devices (ECDs) have been reported, including organic or inorganic species. The judicious combination of both functions of EC and PL in one material was reported for the first time as electrochemically driven photo-switches by Lehn *et al.* in 1993.[6] Then, Audebert and Kim *et al.* proved the possibility of using redox active fluorescent molecules to fabricate devices that can exhibit different PL intensities during electrochemical switching.[7] However, the resulting devices prepared by this approach only possessed moderate electrochemical stability and a low PL contrast ratio due to the ACQ effect. In order to improve the performance to satisfy the requirements for optoelectronic applications, more adaptable materials with redox-active and PL characteristics in the solid state are necessary to be further explored. Several electrofluorochromic (EFC) devices derived from small organic molecules,

[a]*Institute of Polymer Science and Engineering, National Taiwan University, Taipei City 10617, Taiwan. E-mail: gsliou@ntu.edu.tw*
[b]*Department of Chemistry, The Hong Kong University of Science & Technology, Clear Water Bay, Kowloon, Hong Kong, China. E-mail: tangbenz@ust.hk*
[c]*Advanced Research Center for Green Materials Science and Technology, National Taiwan University, Taipei, Taiwan 10617*

†Electronic supplementary information (ESI) available: IR spectra, ^{1}H NMR spectra, and thermal properties. See DOI: 10.1039/c8py00809d

‡These authors contributed equally to this work.

inorganic materials, and high performance polymers have been reported.[8–16] Among them, arylamine-based polymers have been developed rapidly due to their facile processability for the fabrication of solid-state electro-switchable devices.[17–21]

Derivatives of triphenylamine (TPA) have been extensively applied in different optoelectronic applications, including ECDs, OLEDs, and dye-sensitized solar cells (DSSCs).[22–31] These applications could be achieved because the lone pair electrons of nitrogen in TPA can be efficiently oxidized to the cation radical state. In order to improve the poor fluorescence of TPA, some cyano-substituted TPA-based materials (**TPA-CN**) with strong visible emission in the solid state have been designed and synthesized. For example, two AEE- and electroactive cyanoarylamine-containing polyimide (**TPA-CN-PI**) and polyamide (**TPA-CN-PA**) have been prepared by our group and were used to fabricate flexible EFC devices with a high PL contrast ratio from the fluorescent neutral state to the non-fluorescent cation radical oxidized state.[10,30] Accordingly, fluorophores consisting of **TPA-CN** are anticipated to be promising materials with electrochemically dual-switching coloration/emission.

Tetraphenylethene (TPE) is a prototypical and well-known luminogen with AIE characteristics (AIEgen) which has been extensively investigated by the groups of Tang *et al.*[31–39] The central ethylene stator of TPE is surrounded by four peripheral aromatic rotors (phenyl rings). In dilute solutions, the dynamic rotations of the aromatic rotors against the stator around the single-bond axes non-radiatively dissipate the exciton energy. In addition, the central olefinic double bond could be opened in the excited state, generating two diphenylmethylene (DPM) moieties. The friction between their rotational or twisting motions and the solvent media transforms the photonic energy into thermal energy, which also leads to non-emitting relaxation of the excitons. Therefore, the isolated TPE molecules in a dilute solution emit almost no light. Upon aggregate formation, the emission of TPE is rejuvenated or induced by the synergistic effects of the restriction of intramolecular motions in aggregates together with its constrained highly twisted molecular conformation that avoids the occurrence of strong intermolecular π–π stacking interactions. However, its practical application in high-performance EFC devices is restricted greatly by its high oxidation potential. In this regard, exploring a rational design strategy to combine TPE and moieties with a low oxidation potential could be a feasible way to decrease the oxidation potential and consequently improve the electrochemical switching stability of the resulting polymers. Considering the low oxidation potential of the TPA moieties substituted with the electron-donating methoxy group at the *para*-position (**TPA-OMe**),[40–42] **TPA-OMe** is thus possible to readily act as an effective modulator in dual-switching TPE-based EFC systems.

In this paper, we designed and prepared three kinds of polyamides. **TPA-OMe** moieties introduced into the polymer backbone could be expected to reduce the oxidation potential associated with the enhanced electrochemical switching reversibility of the resulting polyamides; **TPA-CN** and TPE units incorporated into the system are responsible for generating a stronger illumination ability. Besides, with the assistance of the counter EC material heptyl viologen (HV), the response time and applied voltage could be further improved. The results in this work indicate that these polyamides are promising candidates to be used to fabricate high-performance EFC devices with electrochromical/electrofluorescent dual-switching behaviors under a low applied voltage.

Experimental section

Materials

4,4′-Diamino-4″-cyanotriphenylamine (**TPA-CN**) and 4,4′-diamino-4″-methoxytriphenylamine (**TPA-OMe**) were prepared according to the literature;[43,44] cyclohexane-1,4-dicarboxylic acid was commercially available, and 4,4′-(1,2-diphenylethene-1,2-diyl)dibenzoic acid (TPE-2COOH) was prepared based on previous studies.[45,46] All other reagents were commercially available and used without further purification. Three TPA-based aromatic polyamides (**TPA-CN-CH**, **TPA-CN-TPE** and **TPA-OMe-TPE**) were prepared by the direct condensation polymerization of the diamines and the dicarboxylic acids. The synthetic route and detailed synthetic procedures are shown in the ESI† with the synthesis of **TPA-OMe-TPE** as an example.

Measurements of polymer properties

Fourier transform infrared (FT-IR) spectra were recorded on a PerkinElmer Spectrum 100 Model FT-IR spectrometer. The inherent viscosities were determined at 0.5 g dL^{-1} using a Tamson TV-2000 viscometer at 30 °C. Gel permeation chromatographic (GPC) analysis was carried out on a Waters chromatography unit interfaced with a Waters 2410 refractive index detector. Two Waters 5 μm Styragel HR-2 and HR-4 columns (7.8 mm I. D. × 300 mm) were connected in series with *N*-methylpyrrolidone (NMP) as the eluent at a flow rate of 0.5 mL min^{-1} at 40 °C and were calibrated with polystyrene standards.

Device fabrication and measurements

EC polymer films were obtained by drop-coating 200 μL of DMAc solution of the polymer sample (2 mg mL^{-1} for the preparation of the film with a thickness of 250 nm) onto an ITO glass substrate (2.5 cm × 3.0 cm × 0.07 cm, 5 Ω per square). The ITO glass was firstly cleaned with water, acetone, and isopropanol, respectively, by ultrasonication each for 15 min. Then the polymer was drop-coated onto an active area (2.0 cm × 2.0 cm) and dried under vacuum to prepare a smooth thin film. In order to obtain a highly transparent semi-gel type electrolyte, 10 wt% poly(methyl methacrylate) (PMMA) (M_w: 120 000) and $LiBF_4$ were plasticized with propylene carbonate (PC); $LiBF_4$ (0.3 g) as the supporting electrolyte and 0.06 g of 0.02 M $HV(BF_4)_2$ were added to the solution of PMMA (0.78 g) in PC (5.5 mL). Two ITO glasses (one of the

glasses was without a polymer film coating) were laminated with thermally cured epoxy resin adhesives using a full-auto dispenser and heated at 120 °C for 6 hours to obtain the devices with a gap of 120 μm (controlled by beaded glasses dispersed in the adhesives) and the active area (2.0 cm × 2.0 cm) of the device was also controlled. Only one tiny hole was left for the devices to inject the electrolyte. After injecting the electrolyte, the devices were sealed with UV-curing adhesive.

Results and discussion

Polymer synthesis and characterization

A novel polyamide **TPA-OMe-TPE** was synthesized by the direct polymerization of **TPA-OMe** and **TPE-COOH** (Scheme S1†). **TPA-CN-CH** and **TPA-CN-TPE** could be obtained according to previous reports.[10,47] The detailed synthetic procedures for **TPA-OMe-TPE** can be found in the ESI.† The thermal properties, inherent viscosity and molecular weight, and the solubility behavior of the synthesized **TPA-OMe-TPE** are summarized in Tables S1, S2 and S3 (the ESI†), respectively. The results indicated that the **TPA-OMe-TPE** possesses high thermal stability and good solubility. It can be dissolved in many aprotic amide solvents such as NMP, DMAc, THF, DMSO, $CHCl_3$, *etc.*, and its solution can be cast into flexible and transparent films. FT-IR and NMR spectra of **TPA-OMe-TPE** are shown in Fig. S1 and S2 (ESI†), respectively. The TGA and DSC traces are shown in Fig. S3 and S4 (ESI†), respectively. The chemical structures of **TPA-CN-CH**, **TPA-CN-TPE** and **TPA-OMe-TPE** and the schematic diagram of the **EFC** device are shown in Fig. 1. The design concept for the structure and property relationship of the high-performance polyamides with different functional groups and the roles of each struc-

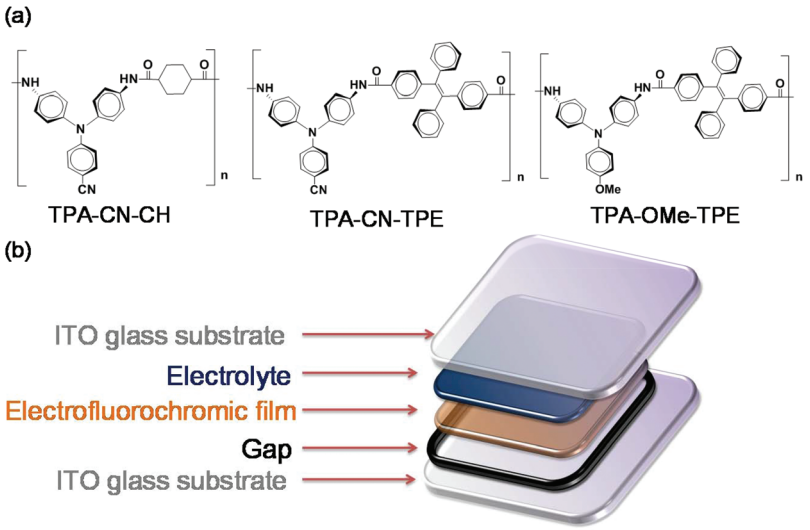

Fig. 1 (a) Chemical structures of **TPA-CN-CH**, **TPA-CN-TPE** and **TPA-OMe-TPE**. (b) Schematic diagram of EFC devices based on three polyamides.

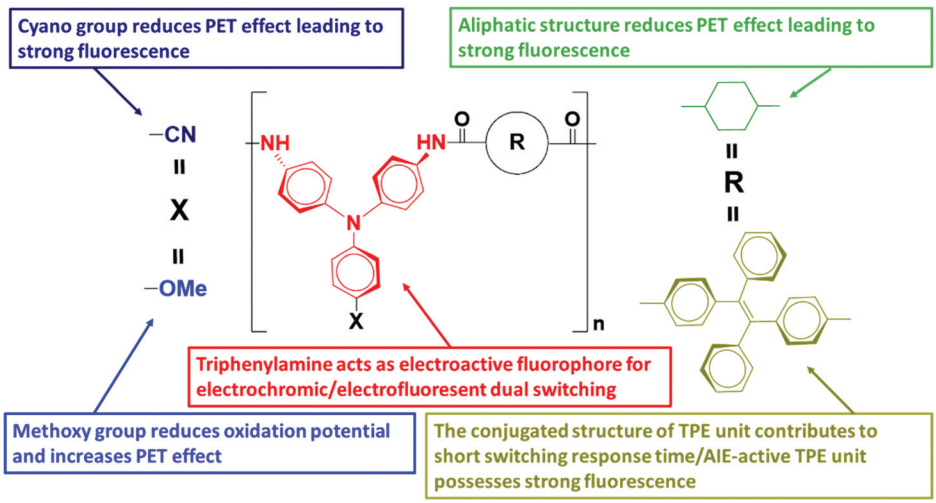

Scheme 1 Design concept for the structure and property relationship of high-performance polyamides with different functional groups.

tural component played in the device performance are shown in Scheme 1.

Electrochromic properties of the devices

The electrochemical behaviors of EFC devices based on **TPA-CN-CH**, **TPA-CN-TPE** and **TPA-OMe-TPE** with/without HV were investigated by cyclic voltammetry (CV). The results as shown in Fig. 2 revealed that with the assistance of HV, the driven potential could be effectively decreased. Typical spectro-electrochemistry of these devices was also investigated and the obtained spectra are shown in Fig. 3. All EFC devices based on these three polyamides are demonstrated to be highly transparent in the neutral form (0 V) and different optical absorption changes could be observed upon oxidation. When the applied voltage was gradually adjusted from 0 to 2.00, 2.10 and 1.75 V for the devices based on **TPA-CN-CH**, **TPA-CN-TPE** and **TPA-OMe-TPE** without HV, respectively, the intensities of their absorption peaks at 517 nm (for **TPA-CN-CH**), 540 nm (for **TPA-CN-TPE**), and 639 nm (for **TPA-OMe-TPE**) in the visible-light region increased accordingly. The absorption peaks of the devices based on **TPA-CN-CH**, **TPA-CN-TPE** and **TPA-OMe-TPE** with the addition of HV showed a similar trend with the increase of the applied voltage. We then studied the EC behaviors and color changes of the devices and the results are shown in Fig. 4a–c. Their corresponding calculated (L^*, a^*, b^*) coordinates with Commission Internationale de I'Eclairage (CIE) in 1976 are depicted in Fig. 4d and e. L^* is the lightness variable of the sample, whereas a^* and b^* correspond to the antagonistic chromatic process of red/green and yellow/blue, respectively. These results suggested that the color of the EFC devices based on **TPA-CN-CH**, **TPA-CN-TPE** and **TPA-OMe-TPE** changed from almost colorless (L^*, 87.43; a^*, −4.96; b^*, 11.77) to light brown (L^*, 54.89; a^*, 6.74; b^*, 17.70); from almost colorless (L^*, 90.58; a^*, −6.80; b^*, 11.70) to brown (L^*, 58.28; a^*, 4.24; b^*, 26.43); and from light yellowish green (L^*, 86.00; a^*, −12.62; b^*, 33.11) to dark green (L^*, 44.27; a^*, −14.42; b^*, 33.14), respectively, after oxidation. The white board was used as a reference for all the measurements.

Electrofluorochromic properties of the devices

Table 1 and Fig. 5 summarize the absorption and PL properties of the obtained polyamides in the solution and solid film states and the corresponding photographs taken under the illumination of 365 nm UV light are provided in Fig. S5 (the ESI†). The results in Table 1 and Fig. 5 clearly indicated that these polyamides are AEE-active materials. As shown in Fig. 5, the solid film of **TPA-CN-CH**, **TPA-CN-TPE** and **TPA-OMe-TPE** showed a high PL quantum yield (Φ_{PL}) of 46%, 16% and 5% with the emitting peaks at 471, 510 and 554 nm, respectively. In the designed structures of these three polyamides, the TPA-OMe moiety owns a stronger electron-donating ability than the TPA-CN unit; meanwhile, the TPE moiety serves as a stronger electron-acceptor than the cyclohexane unit. Therefore, TPA-OMe-TPE was endowed with the strongest photoinduced electron transfer (PET) effect to exhibit the weakest fluorescence.[48–51] For TPA-CN-TPE, the PET effect is reduced as the electron-donating capability of the TPA-CN moiety is weaker than the TPA-OMe unit. Thus, TPA-CN-TPE

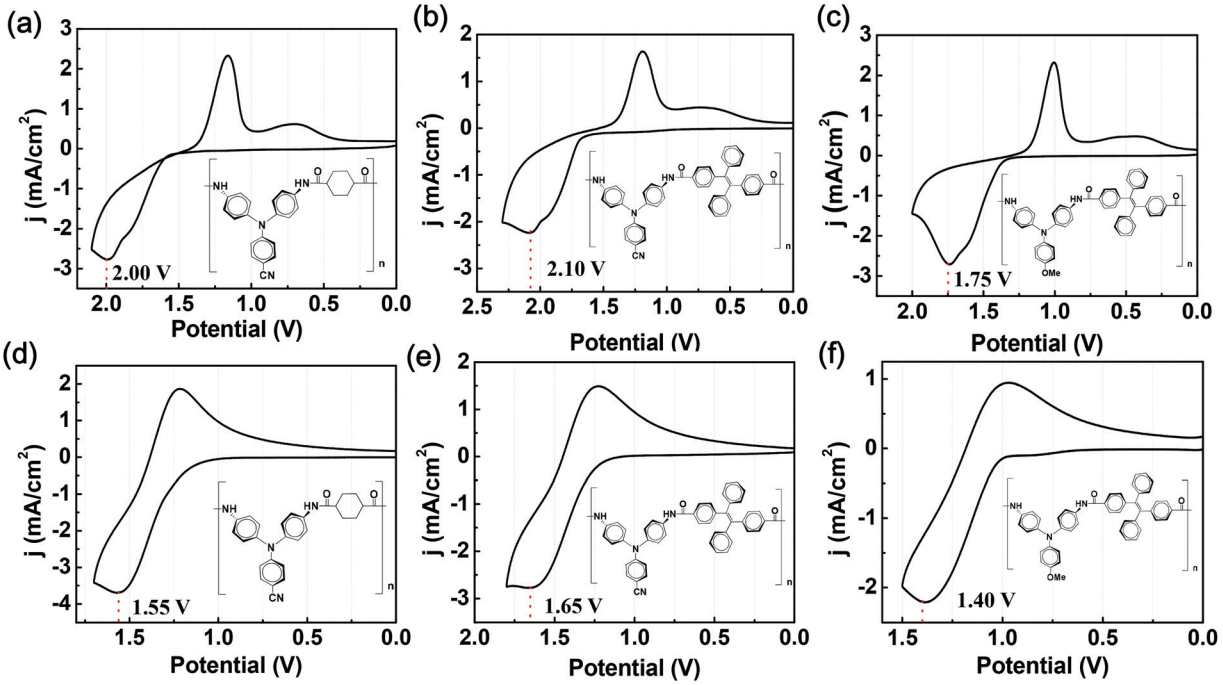

Fig. 2 The electrochemical behaviors of EFC devices based on (a) **TPA-CN-CH**, (b) **TPA-CN-TPE**, (c) **TPA-OMe-TPE**, (d) **TPA-CN-CH**/HV, (e) **TPA-CN-TPE**/HV, and (f) **TPA-OMe-TPE**/HV at a scan rate of 50 mV s^{-1}.

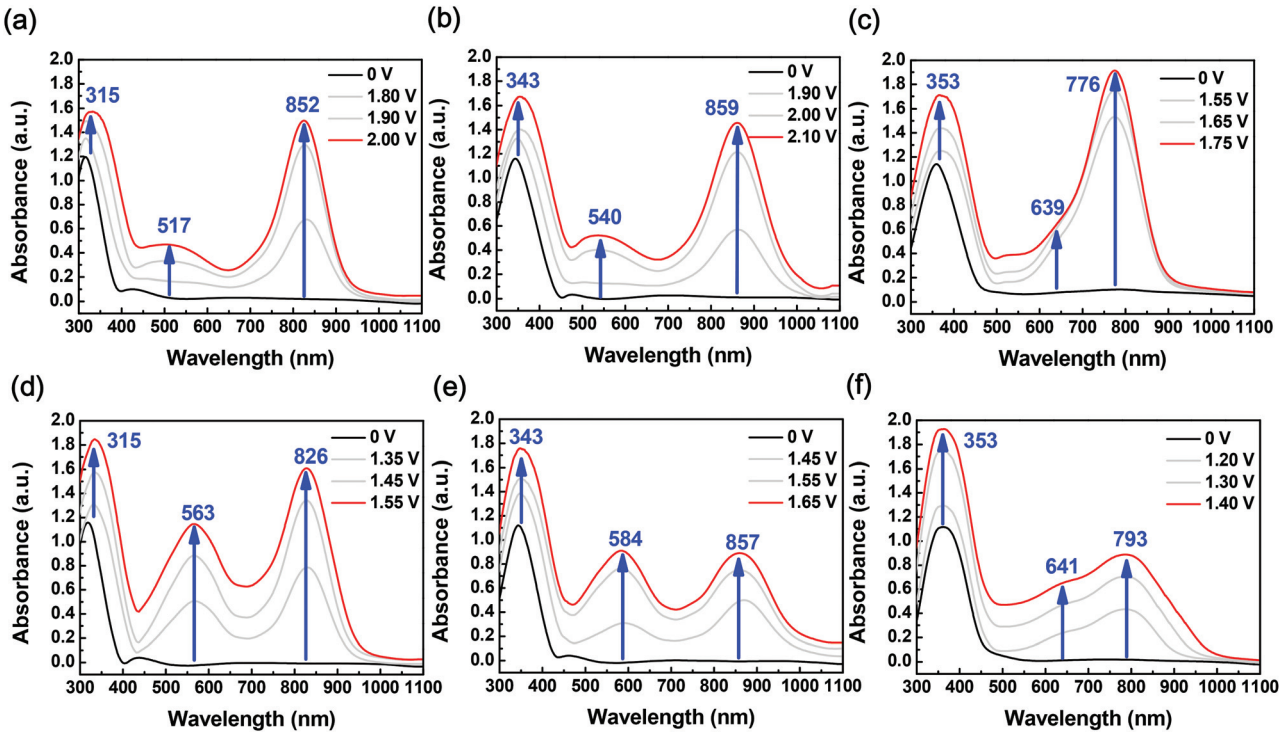

Fig. 3 Spectroelectrochemical spectra of EFC devices based on (a) **TPA-CN-CH**, (b) **TPA-CN-TPE**, (c) **TPA-OMe-TPE**, (d) **TPA-CN-CH**/HV, (e) **TPA-CN-TPE**/HV, and (f) **TPA-OMe-TPE**/HV (a polymer film with a thickness of 200 ± 10 nm).

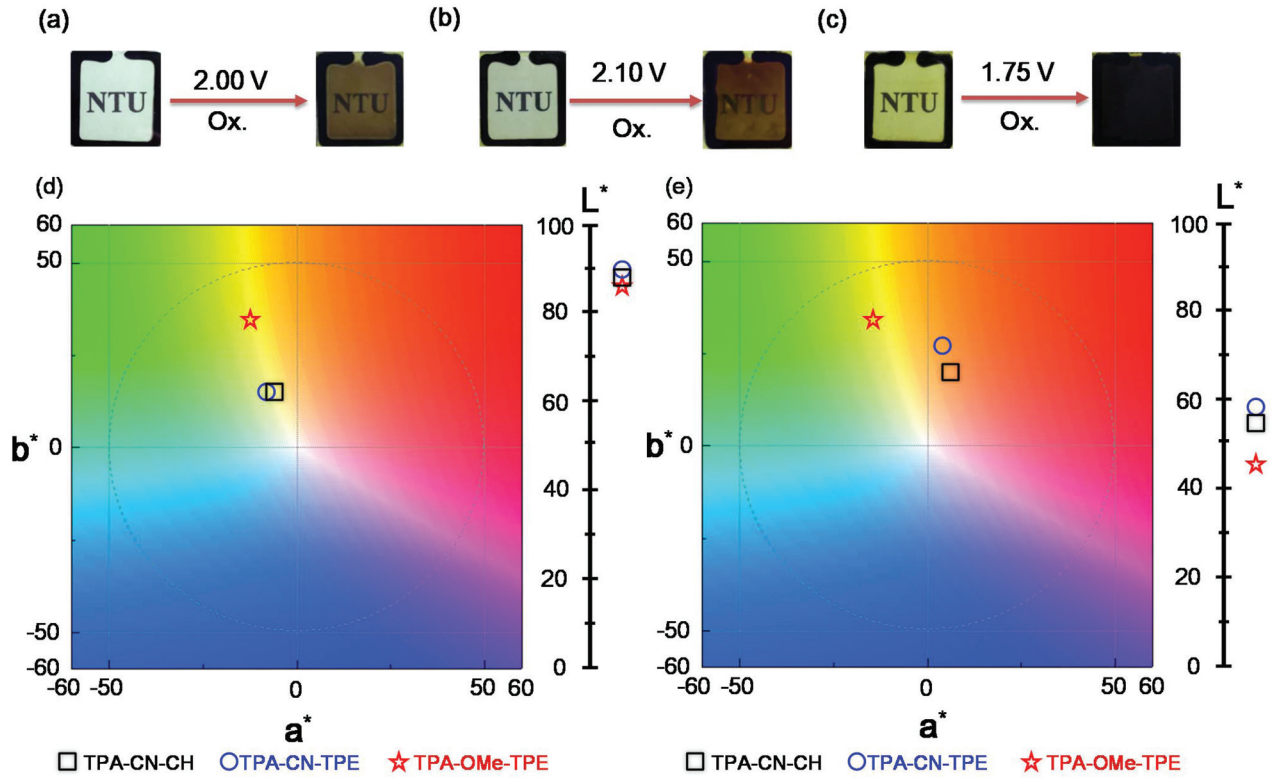

Fig. 4 EC behaviors of devices based on (a) **TPA-CN-CH**, (b) **TPA-CN-TPE** and (c) **TPA-OMe-TPE** with a specific applied voltage for oxidation; CIE 1976 color coordinates of EC devices based on three different polymers in the (d) neutral state and (e) the oxidized state.

Table 1 Optical properties of the polyamides

	NMP (10 μM) solution			Solid film		
Polymer	λ_{abs} [nm]	λ_{em} [a] [nm]	Φ_{PL} [b] [%]	λ_{abs} [nm]	λ_{em} [a] [nm]	Φ_{PL} [c] [%]
TPA-CN-CH	310	492	14	315	470	46
TPA-CN-TPE	339	493	3	343	510	16
TPA-OMe-TPE	347	498	0.8	353	554	5

[a] Samples were excited at λ_{abs} in both the solution and solid states. [b] The quantum yield was measured by using quinine sulfate (dissolved in 1 N H_2SO_4 with a concentration of 10 μM, assuming a photoluminescence quantum efficiency of 0.546) as a standard at 25 °C. [c] PL quantum yields in the solid state were determined using a calibrated integrating sphere.

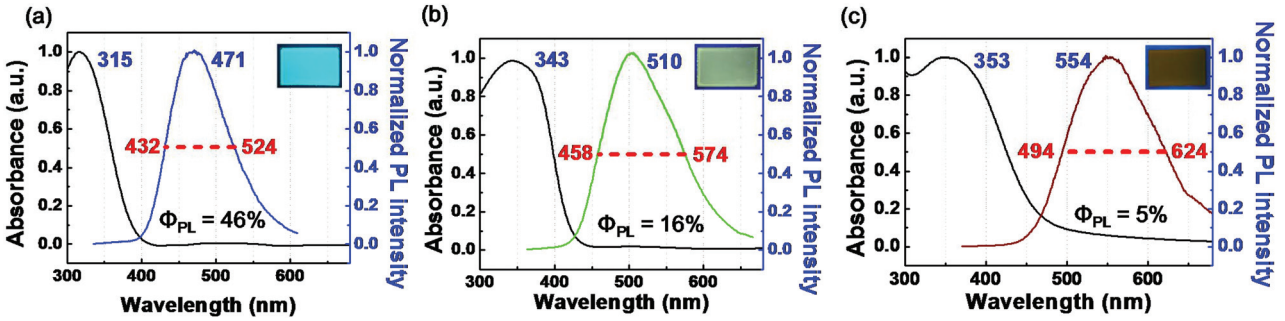

Fig. 5 Photographs taken under the irradiation of 365 nm UV light, absorption spectra, and photoluminescence (PL) spectra of the polymer films of (a) **TPA-CN-CH**, (b) **TPA-CN-TPE** and (c) **TPA-OMe-TPE** together with their associated PL quantum yields. The red dotted lines in the diagrams represent the full width at half maximum (FWHM).

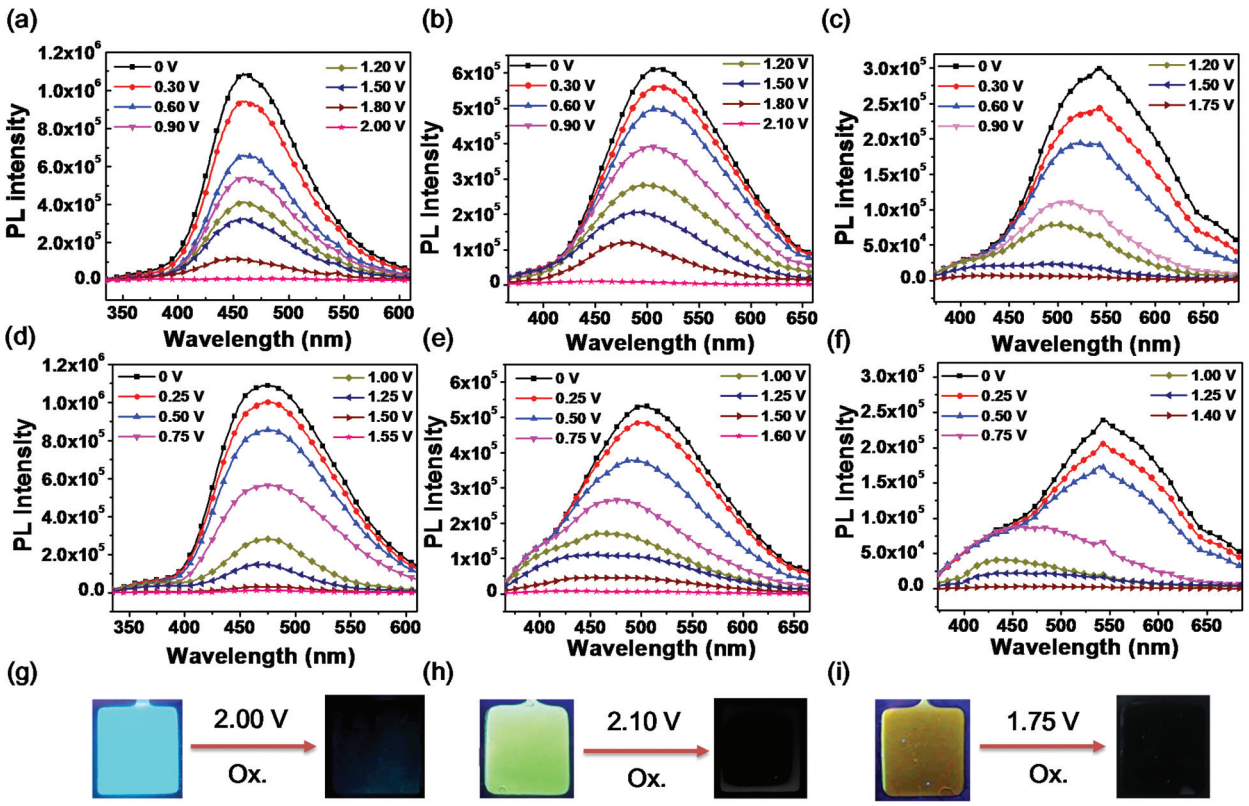

Fig. 6 Diagrams of applied voltage *vs.* PL intensity of EFC devices based on (a) **TPA-CN-CH** (b) **TPA-CN-TPE** (c) **TPA-OMe-TPE** (d) **TPA-CN-CH**/HV (e) **TPA-CN-TPE**/HV (f) **TPA-OMe-TPE**/HV (a polymer film 200 ± 10 nm in thickness; irradiated with 365 nm UV light); (g), (h), and (i) are behaviors of EFC devices based on **TPA-CN-CH**, **TPA-CN-TPE**, and **TPA-OMe-TPE**, respectively, with a specific applied voltage for oxidation.

shows a relatively stronger fluorescence than TPA-OMe-TPE. The presence of an aliphatic moiety (CH) in TPA-CN-CH further reduces the PET process to allow it to show the strongest fluorescence. Although the fluorescence of the TPE-containing polymers is not as strong as that of TPA-CN-CH, the conjugated structure of the TPE unit is likely to contribute to the short switching response time of the corresponding devices. The AIE characteristic of the TPE unit can endow the corresponding polyamides with a more efficient solid-state fluorescence than those composed of conventional conjugated moieties with planar conformations.[52] Meanwhile, a broad emission of full width at half maximum (**FWHM**) could be observed, at 432 to 524 nm for **TPA-CN-CH**, 458 to 574 nm for **TPA-CN-TPE**, and 494 to 624 nm for **TPA-OMe-TPE**. The highly efficient solid-state fluorescence and the good match between the PL spectra and the absorption pattern in the switched-on state of the devices as illustrated in Fig. 3 are beneficial for the achievement of higher fluorescent contrast ratios of the EFC devices.

Furthermore, the peaks could have better matches after adding HV into the system. The PL intensities of these EFC devices with/without HV at various applied voltages are summarized in Fig. 6a–f and different EFC behaviors at a specific applied pulse are also shown in Fig. 6g–i. With the applied pulse changing from 0 to 2 V, the initial bright fluorescence of the EFC device derived from **TPA-CN-CH** obviously quenched into a dark state. Afterwards, the PL intensity could be recovered when the potential was subsequently applied to −2.1 V. The PL contrast ratio (I_{off}/I_{on}) that denotes the ratio between the neutral fluorescent state and the oxidized dark state is determined to be as high as 98, which is much higher than the value reported in a previous study.[8] For EFC devices based on **TPA-CN-TPE** and **TPA-OMe-TPE**, their fluorescence can also be quenched to a dark state by applying a voltage from 0 to 2.1 V and from 0 to 1.75 V, respectively. The quenched fluorescence of **TPA-CN-TPE** and **TPA-OMe-TPE** at 2.1 V and 1.75 V could be attributed to their cation radicals with absorption peaks at around 540 and 639 nm, respectively (Fig. 3). As shown in Fig. 7, the redox scanning at different cycle times was investigated during the fluorescence switching procedure for elucidating the response behavior of EFC devices based on **TPA-CN-CH**, **TPA-CN-TPE** and **TPA-OMe-TPE** with/without HV. With repetitive applied voltage pulses between the neutral state and the oxidized state, denoting fluorescence and non-fluorescence, the devices showed reversible fluorescence switching properties. The response time of fluorescence estimated at 90% of the full switching process of **TPA-CN-CH**, **TPA-CN-TPE** and **TPA-OMe-TPE** was monitored at 471 nm, 510 nm and 554 nm, respectively. The response time of the EFC devices based on **TPA-CN-CH**, **TPA-CN-TPE** and **TPA-OMe-TPE** is 8.6, 7.1, and 6.5 s, respectively. Moreover, the PL contrast ratio decreased from 98 to 15 for **TPA-CN-CH**, 64 to 8 for **TPA-CN-TPE**, and 48 to 10 for **TPA-OMe-TPE** with decreasing switching cyclic time from 360 s to 10 s, correspondingly. Furthermore, long-term stability and reversibility of the resulting EFC devices were also investigated by measuring the PL

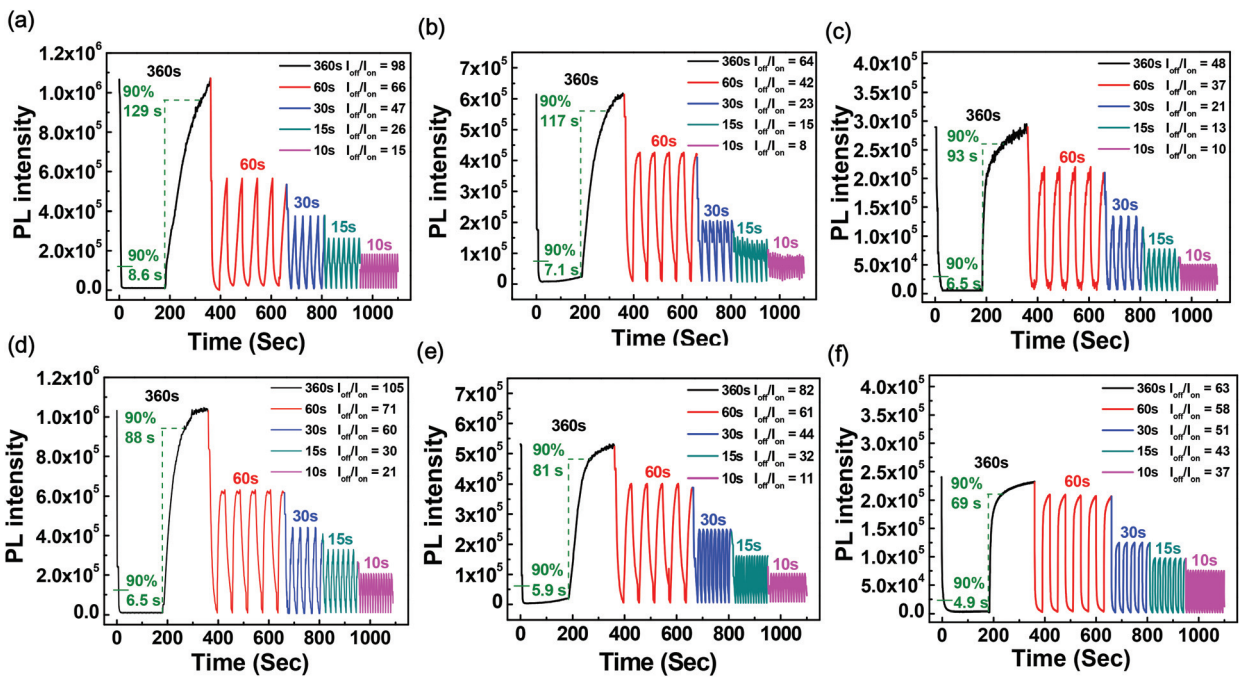

Fig. 7 Estimation of the fluorescence switching time at different step cycle times of 360, 60, 30, 20, and 10 s of (a) **TPA-CN-CH** between 2.0 V and −2.1 V monitored at 471 nm (λ_{ex} = 315 nm), (b) **TPA-CN-TPE** between 2.1 V and −2.2 V monitored at 510 nm (λ_{ex} = 343 nm), and (c) **TPA-OMe-TPE** between 1.75 V and −1.85 V monitored at 554 nm (λ_{ex} = 353 nm), (d) **TPA-CN-CH**/HV between 1.4 V and −1.5 V monitored at 471 nm (λ_{ex} = 315 nm), (e) **TPA-CN-TPE**/HV between 1.4 V and −1.5 V monitored at 510 nm (λ_{ex} = 343 nm), and (f) **TPA-OMe-TPE**/HV between 1.4 V and −1.5 V monitored at 554 nm (λ_{ex} = 353 nm).

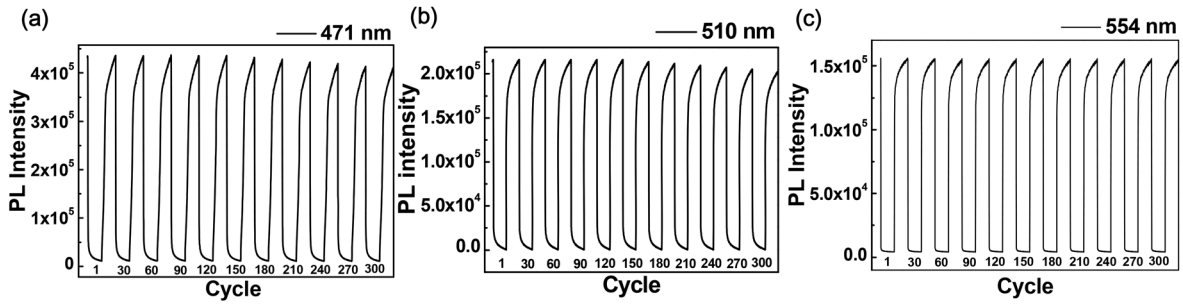

Fig. 8 EFC switching of devices based on (a) **TPA-CN-CH** (b) **TPA-CN-TPE** and (c) **TPA-OMe-TPE** with a cycling time of 30 s.

intensity as a function of switching cycles as shown in Fig. 8. The recovery of EFC devices based on **TPA-CN-CH**, **TPA-CN-TPE** and **TPA-OMe-TPE** after 300 cycles was 95, 94 and 98%, respectively, implying their excellent EFC stability. The relatively better EFC stability of **TPA-OMe-TPE** could be ascribed to its lower oxidation potential in comparison with the cases of **TPA-CN-CH** and **TPA-CN-TPE**.

The addition of HV was demonstrated to be favourable for the further improvement of the device performance. EFC devices based on **TPA-CN-CH**/HV, **TPA-CN-TPE**/HV and **TPA-OMe-TPE**/HV revealed a lower oxidation potential (1.55, 1.65 and 1.40 V) than those prepared without HV (2.00, 2.10 and 1.75 V) (Fig. 2d–f). As shown in Fig. 9, this trend could be ascribed to the unique characteristics of the ambipolar EC system where HV^{2+} has the capability to catch the electrons from TPA moieties to form HV^{+} during oxidation and then could release the electrons back to TPA^{+} in the reduction process. The spectroelectrochemical absorption spectra of devices derived from **TPA-CN-CH**/HV, **TPA-CN-TPE**/HV and **TPA-OMe-TPE**/HV (Fig. 3d–f) revealed similar absorption patterns to the devices without HV in the neutral state (0 V), whereas a more distinctly enhanced absorption band with peaks at 563, 584 and 641 nm could be observed, respectively, due to the contribution from the reduction state of HV. Such a difference resulted in better optical matches between the absorption in the switched-on state and the PL emission wavelength range of the HV-doped polyamides. Therefore, the PL contrast ratio was expected to be promoted by more effective quenching. Indeed, with the assistance of HV, **TPA-CN-TPE**/HV and **TPA-OMe-TPE**/HV-based EFC devices exhibited much higher I_{off}/I_{on} values than those without HV (Fig. 7d–f). The **TPA-CN-CH**/HV-based EFC device displayed the largest PL contrast ratio because it possesses the strongest luminescence intensity as mentioned above. Moreover, the redox cycles of the **TPA-OMe-TPE**/HV-based EFC device associated with the fluorescence switching procedure as shown in Fig. 7f exhibited

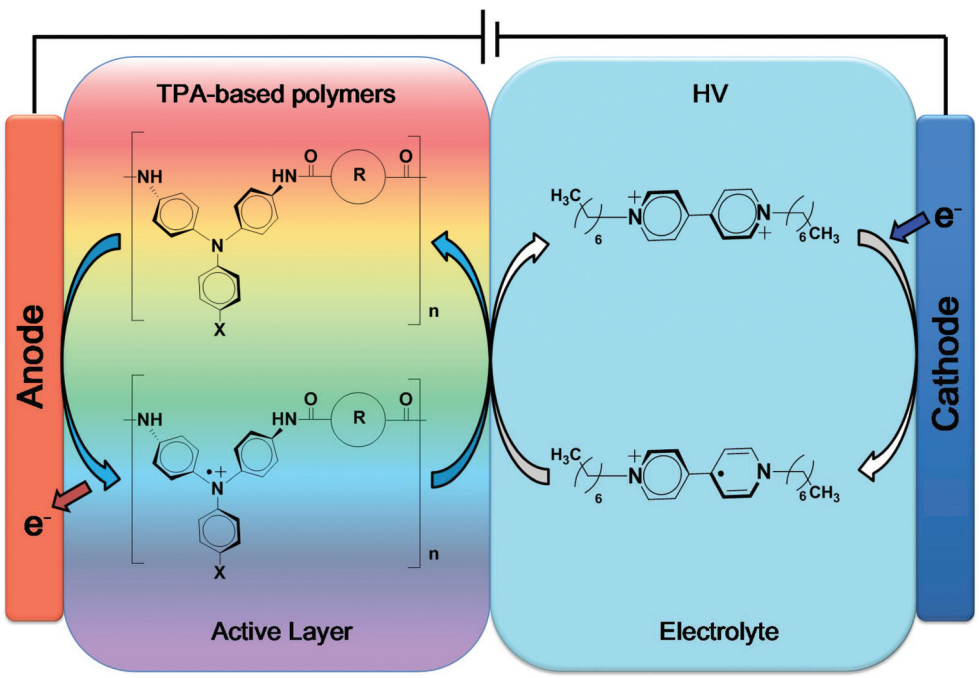

Fig. 9 Working principle of TPA-based polyamides/HV EFC devices (X = cyano or methoxy group; R = cyclohexane or tetraphenylethene).

the largest increase in terms of the I_{off}/I_{on} values monitored at 554 nm, between 1.40 V and −1.50 V when compared with the corresponding device without adding HV (Fig. 7c), demonstrating the remarkable effect of HV on the EFC performance. Especially for the cases of a shorter cycling time, the I_{off}/I_{on} values could be promoted from 21 to 51, 13 to 43, and 10 to 37 related to the cycling times of 30, 15, and 10 s, respectively. Thus, high-performance EFC devices having an excellent switching response ability and a higher PL contrast ratio could be effectively achieved.

Conclusions

In this research, three kinds of polyamides with AIE-active TPE and electro-active TPA moieties were successfully prepared. The introduction of the electron-donating methoxy substituent into the TPA moiety could effectively reduce the oxidation potential associated with an enhanced electrochemical switching ability of the resulting polyamides. Meanwhile, TPA with the cyano group and TPE moieties were incorporated into the polyamides for obtaining an enhanced illumination capability. We demonstrate that these aromatic polyamides could display electrochromic/electrofluorescent dual-switching behavior with a low trigger voltage and short response time. EFC devices based on **TPA-CN-CH**/HV with a high photoluminescence quantum yield of 46% as the active layer revealed the highest contrast ratio (I_{off}/I_{on}) of 105. Besides, with the addition of HV into the system as a counter EC layer to balance the charges, the prepared **TPA-OMe-TPE**/HV-based EFC device exhibits the shortest response time of less than 4.9 s in addition to lowering the oxidation potential. It is a facile and feasible approach to achieve high-performance EFC devices by judicious combination of EC- and PL-active moieties into the target polymers.

Conflicts of interest

There are no conflicts to declare.

Acknowledgements

This work was financially supported by the "Advanced Research Center for Green Materials Science and Technology" from The Featured Area Research Center Program within the framework of the Higher Education Sprout Project by the Ministry of Education (107L9006) and the Ministry of Science and Technology in Taiwan (MOST 107-3017-F-002-001 and 104-2113-M-002-002-MY3).

Notes and references

1 J. Luo, Z. Xie, J. W. Y. Lam, L. Cheng, H. Chen, C. Qiu, H. S. Kwok, X. Zhan, Y. Liu, D. Zhu and B. Z. Tang, *Chem. Commun.*, 2001, **18**, 1740.
2 J. Mei, N. L. C. Leung, R. T. K. Kwok, J. W. Y. Lam and B. Z. Tang, *Chem. Rev.*, 2015, **115**, 11718.
3 J. Yang, J. Huang, Q. Li and Z. Li, *J. Mater. Chem. C*, 2016, **4**, 2663–2684.
4 Q. Li and Z. Li, *Adv. Sci.*, 2017, **4**, 1600484.
5 J. R. Platt, *J. Chem. Phys.*, 1961, **34**, 862.
6 V. Goulle, A. Harriman and J.-M. Lehn, *J. Chem. Soc., Chem. Commun.*, 1993, 1034.
7 Y. Kim, E. Kim, G. Clavier and P. Audebert, *Chem. Commun.*, 2006, 3612.
8 S. Seo, Y. Kim, Q. Zhou, G. Clavier, P. Audebert and E. Kim, *Adv. Funct. Mater.*, 2012, **22**, 3556.
9 Y. X. Yuan, Y. Chen, Y. C. Wang, C. Y. Su, S. M. Liang, H. Chao and L. N. Ji, *Inorg. Chem. Commun.*, 2008, **11**, 1048.
10 H. J. Yen and G. S. Liou, *Chem. Commun.*, 2013, **49**, 9797.
11 P. Audebert and F. Miomandre, *Chem. Sci.*, 2013, **4**, 575.
12 J. W. Sun, Y. N. Chen and Z. Q. Liang, *Adv. Funct. Mater.*, 2016, **26**, 2783.
13 H. Al-Kutubi, H. R. Zafarani, L. Rassaei and K. Mathwig, *Eur. Polym. J.*, 2016, **83**, 478.
14 E. Puodziukynaite, J. L. Oberst, A. L. Dyer and J. R. Reynolds, *J. Am. Chem. Soc.*, 2012, **134**, 968.
15 K. Kanazawa, K. Nakamura and N. Kobayashi, *J. Phys. Chem. A*, 2014, **118**, 6026.
16 K. Kanazawa, K. Nakamura and N. Kobayashi, *Sol. Energy Mater. Sol. Cells*, 2016, **145**, 42.
17 C. P. Kuo, Y. S. Lin and M. K. Leung, *J. Polym. Sci., Part A: Polym. Chem.*, 2012, **50**, 5068.
18 C. P. Kuo and M. K. Leung, *Phys. Chem. Chem. Phys.*, 2014, **16**, 79.
19 C. P. Kuo, C. L. Chang, C. W. Hu, C. N. Chuang, K. C. Ho and M. K. Leung, *ACS Appl. Mater. Interfaces*, 2014, **6**(20), 17402.
20 J. H. Wu and G. S. Liou, *Adv. Funct. Mater.*, 2014, **24**, 6422.
21 J. W. Sun and Z. Q. Liang, *ACS Appl. Mater. Interfaces*, 2016, **8**, 18301.
22 Y. Shirota, *J. Mater. Chem.*, 2005, **15**, 75.
23 P. Cias, C. Slugovc and G. Gescheidt, *J. Phys. Chem. A*, 2011, **115**, 14519.
24 A. Mishra, M. K. R. Fischer and P. Bauerle, *Angew. Chem., Int. Ed.*, 2009, **48**, 2474.
25 G. Zhang, H. Bala, Y. Cheng, D. Shi, X. Lv, Q. Yu and P. Wang, *Chem. Commun.*, 2009, **16**, 2198.
26 T. Kurosawa, T. Higashihara and M. Ueda, *Polym. Chem.*, 2013, **4**, 16.
27 H. J. Yen and G. S. Liou, *Polym. J.*, 2016, **48**, 117.
28 H. J. Yen and G. S. Liou, *Polym. Chem.*, 2012, **3**, 255.
29 S. H. Hsiao and S. W. Lin, *J. Mater. Chem. C*, 2016, **4**, 1271.
30 C. W. Hu, K. M. Lee, K. C. Chen, L. C. Chang, K. Y. Shen, S. C. Lai, T. H. Kuo, C. Y. Hsu, L. M. Huang, R. Vittal and K. C. Ho, *Sol. Energy Mater. Sol. Cells*, 2012, **99**, 135.
31 J. Mei, Y. Hong, J. W. Y. Lam, A. Qin, Y. Tang and B. Z. Tang, *Adv. Mater.*, 2014, **26**, 5429–5479.
32 Y. Hong, J. W. Y. Lam and B. Z. Tang, *Chem. Commun.*, 2009, 4332.
33 Y. Hong, J. W. Y. Lam and B. Z. Tang, *Soc. Rev.*, 2011, **40**, 5361.

34 R. Hu, N. L. Leung and B. Z. Tang, *Chem. Soc. Rev.*, 2014, **43**, 4494.
35 M. Wang, G. Zhang, D. Zhang, D. Zhu and B. Z. Tang, *J. Mater. Chem.*, 2010, **20**, 1858.
36 J. Liu, J. W. Y. Lam and B. Z. Tang, *J. Inorg. Organomet. Polym. Mater.*, 2009, **19**, 249.
37 Z. Zhao, J. W. Y. Lam and B. Z. Tang, *J. Mater. Chem.*, 2012, **22**, 23726.
38 D. Ding, K. Li, B. Liu and B. Z. Tang, *Acc. Chem. Res.*, 2013, **46**, 2441.
39 R. T. K. Kwok, C. W. T. Leung, J. W. Y. Lam and B. Z. Tang, *Chem. Soc. Rev.*, 2015, **44**, 4228.
40 H. J. Yen and G. S. Liou, *Chem. Mater.*, 2009, **21**, 4062.
41 H. J. Yen, H. Y. Lin and G. S. Liou, *Chem. Mater.*, 2011, **23**, 1874.
42 H. J. Yen, C. J. Chen and G. S. Liou, *Adv. Funct. Mater.*, 2013, **23**, 5307.
43 H. J. Yen, C. J. Chen and G. S. Liou, *Chem. Commun.*, 2013, **49**, 630.
44 C. W. Chang, G. S. Liou and S. H. Hsiao, *J. Mater. Chem.*, 2007, **17**, 1007.
45 B. Z. Tang, Y. N. Hong, S. J. Chen and T. K. Kwok, *US* 20120172296A1, 2012.
46 B. Z. Tang, W. Y. Lam, J. Z. Liu and F. Mahtab, *US* 20130210047A1, 2013.
47 S. W. Cheng, T. Han, T. Y. Huang, Y. H. Chang Chien, C. L. Liu, B. Z. Tang and G. S. Liou, *ACS Appl. Mater. Interfaces*, 2018, **10**, 18281–18288.
48 E. V. Anslyn and D. A. Dougherty, *Modern Physical Organic Chemistry*, University Science Books, Sausalito, CA, 2005, pp. 955–958.
49 A. P. De Silva, T. S. Moody and G. D. Wright, *Analyst*, 2009, **134**, 2385–2393.
50 H. Deng, Z. He, J. W. Lam and B. Z. Tang, *Polym. Chem.*, 2015, **6**, 8297–8305.
51 W. Zhang, Z. Ma, L. Du and M. Li, *Analyst*, 2014, **139**, 2641–2649.
52 C. W. Chang, G. S. Liou and S. H. Hsiao, *J. Mater. Chem.*, 2007, **17**, 1007–1015.